WOOD FAILURE UNDER TORSIONAL LOADING AS A FUNCTION OF TEMPERATURE

Zoltan Koran

Professor
Wood and Paper Science, Université du Québec à Trois-Rivières
C.P. 500, Trois-Rivières, Québec, Canada G9A 5H7

ABSTRACT

Cylindrical wood bars were twisted through a 360-degree rotation in a standard torsiometer in glycerine at 20, 60, 100, and 140 C temperatures. The torsional load-deformation curves were plotted for each specimen, and the strain and stress values were calculated at each temperature. The failure zones were studied by light and electron microscopic techniques.

It was found that failure occurs in the radial plane of wood, mostly in the outer region of the bar, as a result of torsional shear stresses acting in the same plane. The temperature dependence of torsional strain is expressed in the form of a characteristic curve, the peak value falling at 100 C and the high rate increase occurring in the range 20–100 C.

Keywords: Wood failure, temperature, red spruce, balsam fir, torsion.

INTRODUCTION

The mechanical defibration of wood is accomplished under the simultaneous cyclic action of the combination of tensile, compressive, and shear stresses. In order to determine the relative role of each type of stress on mechanical fiber separation, a number of investigations have been undertaken under well-controlled experimental conditions.

An initial series of fundamental studies has involved fiber separation in pure tensile failure. These have already been reported in the literature (Koran 1966, 1967a, b, 1979, 1981). Some aspects of these investigations have been extended to commercial, thermomechanical pulping (Koran 1970; Koran et al. 1978). Other related studies are presently in progress.

It is now well recognized that the action of shear stress plays a major role in mechanical defibration. This type of stress may develop in wood as a result of tensile, compressive, and torsional loading. The chips between the refiner plates, for example, are subjected repeatedly to a combination of such stresses. The possible rolling action of wood particles between the plates proposed by Atack (1980) is believed to involve various degrees of torsional deformations and failures. The importance of torsional loading in mechanical defibration has also been recognized by previous researchers (Hoglund and Tistad 1973; Hoglund et al. 1976; Vickstrom and Hammar 1979; Vickstrom and Nelson 1980).

The objective of the present investigation is to identify the existing stress types in torsional loading, study the resulting failures, and evaluate the results in terms of stress and strain relationships as a function of temperature.

Symbols	Units	Nomenclature—definitions
T	N·m	Torque; T_a = applied torque
T_0	N·m	Torque at the elastic limit
T_1	N·m	Ultimate torque; T_r = resisting torque
τ_0, τ_1	MPa	Shearing stress at T_0 and T_1
τ_t, τ_L	MPa	Transverse and longitudinal shear stresses
σ_t	MPa	Tensile stress on oblique planes
σ_c	MPa	Compressive stress on oblique planes
θ	radians	Angle of twist
γ_0	radians	Elastic shearing strain at T_0
γ_1	radians	Inelastic shearing strain at T_1
D	cm	Diameter of cylinder; L = length
Z	cm^3	Polar section modulus; r = radius
J	cm^4	Polar moment of inertia
ρ	cm	Radial distance from the neutral axis

MATERIALS AND METHODS

Cylindrical wood specimens were prepared from freshly felled red spruce (*Picea rubra* (Link.)) and balsam fir (*Abies balsamea* (L., Mill)) trees. The shape of a test specimen is illustrated in Fig. 1B. These were one inch in diameter and 3.5 inches long. All cylindrical rods of uniform circular cross section were saturated with glycerine under vacuum at 20 C for 10 days. The torsion tests were carried out on a bench mounting torsion machine (Fig. 1).

The Tecquipment torsion machine consists of a rigid base (A), a fixed headstock (B), and a manually operated straining head (C). This, in turn, is equipped with a handwheel (HW) for applying the torsional load and with two protractor scales (N and M) to measure the angular displacement of the specimen.

The torsion testing machine was equipped with a custom-made conditioning chamber enclosing the jaws, the sample, a quartz heating element, a stirrer and a thermometer. Before each test, the sample rod was preconditioned in glycerine to the desired temperatures, 20, 60, 100, and 140 C. Four test specimens were tested at each temperature (Table 1).

Glycerine was selected because it is miscible with water and it possesses similar physical properties. Since it has a high boiling point (290 C), it replaces water in wood; as a result the cell wall remains in a swollen state. Thus, the use of glycerine enabled torsional testing above the boiling point of water, without the necessity of developing a rather complicated pressurized conditioning chamber to enclose the jaws and the specimen. A previous study (Koran 1979) revealed no significant difference between the softening effects of glycerine and water on wood up to 100 C.

During the torsion test, the specimen was held in the free end of the shaft assembly. The torsional load was applied at a uniform strain rate of 15 degrees per minute through a complete turn of 360 degrees, normal to the long axis of the specimen. The torque applied to the specimen (S) by the handwheel (HW)
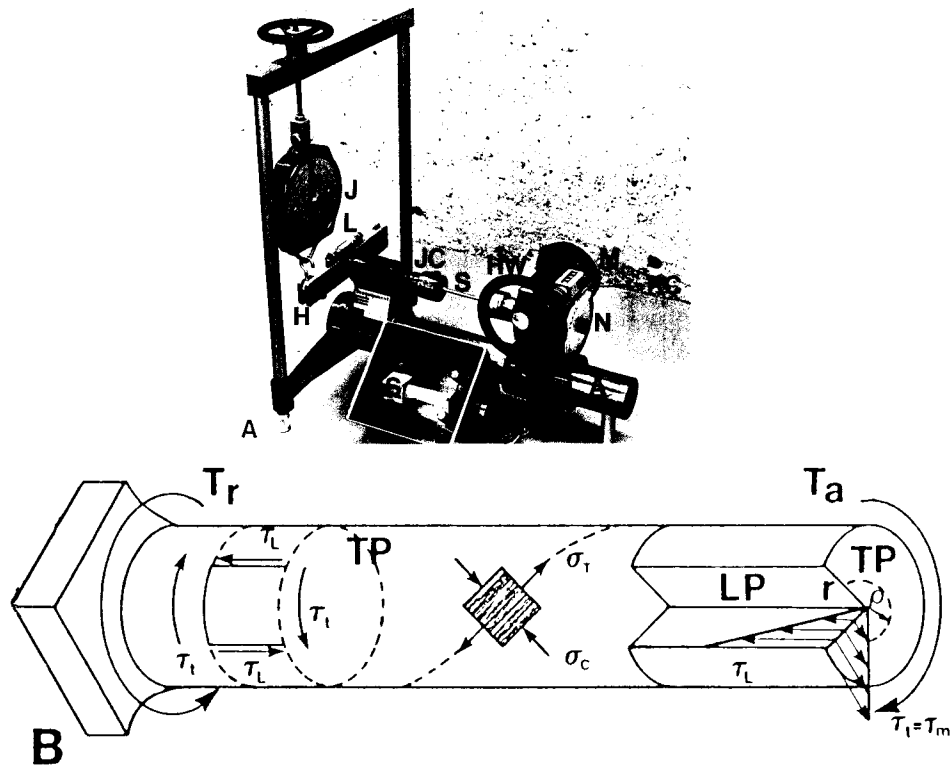
FIG. 1.   A. The Tecquipment torsion testing machine. B. The torsional test specimen showing the stress types developed in it.

was transmitted to a spring balance (J) by the torque arm (H). The spring balance measured the torque applied directly in the N·m units, which in turn was plotted as a function of angular deformation.

The deformation of the cylindrical solid bar is expressed in terms of shearing strain. This varies linearly with the distance along the radius; it goes from zero

TABLE 1.   Applied torque (T_t) and the corresponding deformation (Q) as a function of angular deformation.

| Sample no.	Species of wood	Temperature, C 20		60		100		140	
		Balsam fir	Red spruce	Balsam fir	Red spruce	Balsam fir	Red spruce	Balsam fir	Red spruce
1	Torque, N·m	27.0	24.0	15.6	20.0	10.6	11.9	6.0	6.8
	Angle, degrees	17	26	26	28	37	44	32	36
2	Torque, N·m	25.9	24.6	15.9	16.9	10.5	12.4	7.1	6.0
	Angle, degrees	15	26	28	36	35	40	26	42
3	Torque, N·m	26.0	23.3	19.2	20.0	13.5	10.4	5.9	6.2
	Angle, degrees	16	24	28	34	33	42	26	30
4	Torque, N·m	26.4	—	18.5	17.0	11.4	10.9	—	7.1
	Angle, degrees	19	—	30	30	27	48	—	28
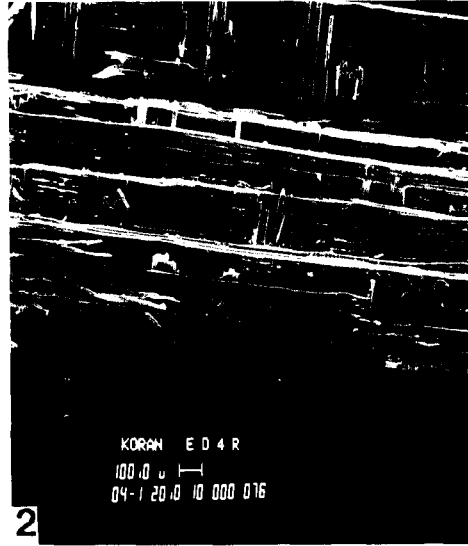
FIG. 2.   A typical example of torsional failure showing fracture in the radial plane of wood.

at the neutral axis ($\rho = 0$) to γ maximum at the surface of the bar ($\rho = r$). Furthermore, the strain at any point along the length of the twisted bar is directly proportional to the distance from its fixed end and is expressed with the equation $\gamma = QD/2L$.

RESULTS AND DISCUSSION

Stress type developed in a torsional bar

When a cylindrical solid bar is subjected to torsional loading, four types of stresses are developed in it. These are the transverse shear stress (τ_t), the complementary longitudinal shear stress (τ_l), and the normal tensile (σ_L) and compressive (σ_c) stresses acting on the oblique planes. These stresses are illustrated in Fig. 1B.

The shear stress generated by elastic loading in a transverse plane is linearly proportional to the corresponding shear strain (γ), as well as to the distance (ρ) from the center of the bar. Thus τ_t increases from zero at its neutral axis to τ maximum on its periphery, as illustrated graphically in Fig. 1B. The direction of τ_t is perpendicular to the direction drawn through the point. The magnitude of τ_t at failure (Fig. 2) is calculated with the following formula:

$$\tau_1 = \frac{T_1}{Z} = \frac{16T_1}{\pi D^3} \qquad \text{where } Z = \frac{\pi D^3}{16} \qquad (1)$$

Since the elastic torsion formula is based on Hooke's law, it applies only up to the proportional limit of the bar (T_0; Fig. 3). Beyond this point the same formula is nevertheless used to calculate an approximate value of the shear stress designated by τ_1 at T_1 (Fig. 3). This parameter is commonly called by such names as fictitious shearing stress, ultimate shear stress, or maximum shear stress and
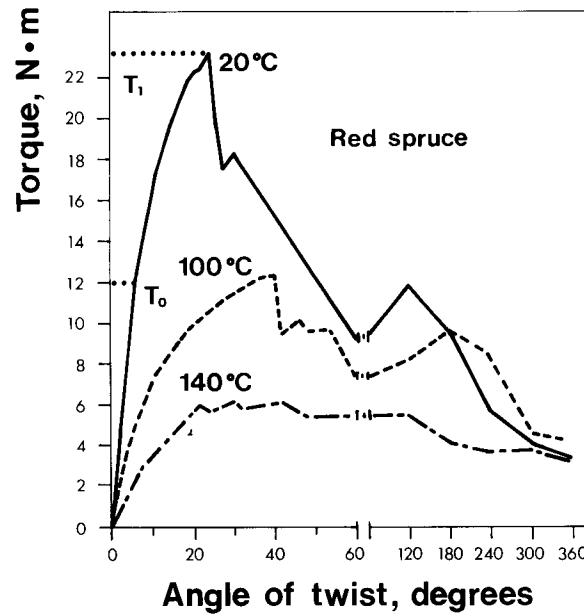
FIG. 3. Torque-deformation curves.

it is even referred to as the modulus of rupture. The shear stresses are calculated at T_0 and T_1 (Fig. 3) and are plotted in Fig. 4A as a function of temperature.

It is recognized that at any point in the stressed bar, τ_L is accompanied by a longitudinal shear stress designated by $\tau_{L'}$. These shearing stresses act on mutually perpendicular planes and are equal in magnitude. This condition holds even though the complementary stresses (σ_t and σ_c) act at the same point on planes that bisect the angles between the planes on which the shearing stresses act.

Torsional shear stress as a function of temperature

The torsional shear stresses determined at T_0 and T_1 are plotted in Fig. 4A as a function of testing temperature for both red spruce and balsam fir. Every point in this figure is the average of four tests and was calculated from the data of Table 1 by Eq. 1.

Figure 4 shows that τ_1 is almost double the value of τ_0. In fact, the average ratio of τ_1/τ_0 is 1.9. This high ratio proves that wood behaves like a ductile material even at 20 C ($\tau_1/\tau_0 = 1.7$), but especially so at high temperatures ($\tau_1/\tau_0 = 2.2$). This is due to the softening effect of glycerine (or water) on lignin in the swollen state.

Figure 4A further shows that τ_0 decreases from an average of 46 kg/cm^2 to 9.2 kg/cm^2 in the temperature range 20–140 C. This corresponds to an 80% decrease in the case of τ_0 and to a similar 75% decrease in τ_1. The above values imply a significant reduction in the resistance of wood to torsional shear stress as a result of temperature increase. This in turn implies a corresponding decrease in the resistance of wood to defibration owing to the cumulative softening effect of lignin and hemicelluloses in the temperature range 20–140 C.
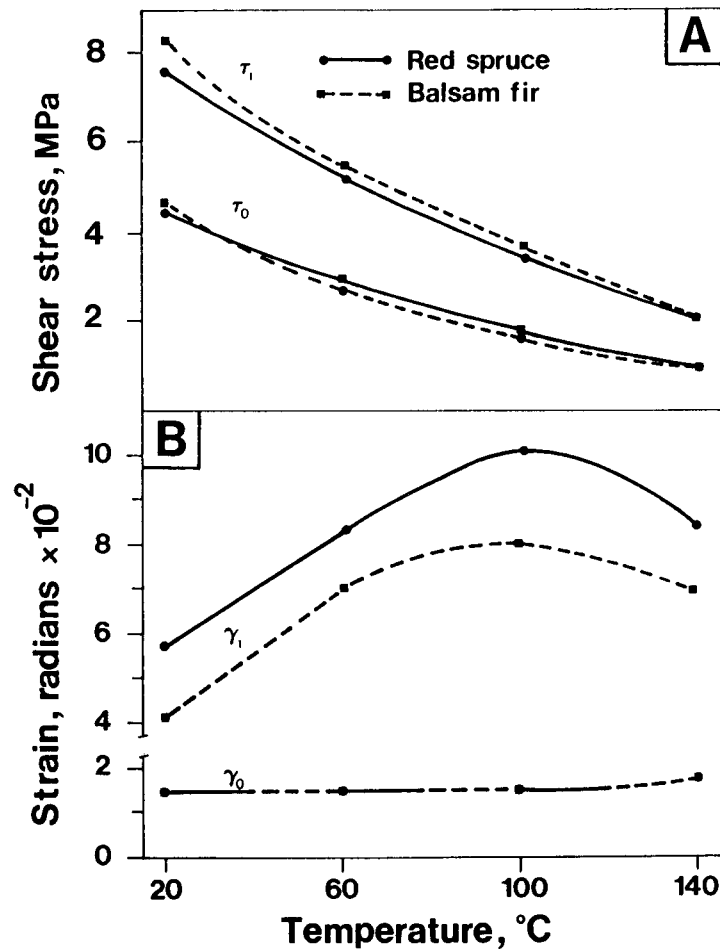
FIG. 4.   Torsional shear stress and strain as a function of temperature.

It is also apparent that the curves tend to level off as the temperature approaches 140 C. A similar phenomenon was observed in perpendicular-to-grain tensile failure (Koran 1979). This implies that additional heating beyond 140 C will have little additional effect on the shear stress.

Strain (γ) in torsional loading (Fig. 4B)

The test specimen illustrated in Fig. 1B is fixed at one end and is twisted at its other end in pure torsion about its longitudinal axis through a complete rotation of 360 degrees. As a result, a chosen point at the extreme end of the 9-cm-long bar (Fig. 1B) is displaced by 360 degrees.

The temperature dependence of the shearing strain is shown in Fig. 4B. Every point on this figure is the average of four experimental values calculated from the data of Table 1. The inelastic strain γ_i is represented by a curve that has its maximal value at 100 C and two descending parts on the sides. Similar curves were obtained in tensile failure (Koran 1979).

In the case of red spruce, the strain increases by 77% in the temperature range 20–100 C and then it decreases by 17% at 140 C. The corresponding changes are respectively 95% and 14% for balsam fir.

The highest rate of change (1%/C) occurs on the low temperature side of the 100 C peak. This can be attributed to the progressive softening of the hemicellulose and lignin, as a result of the temperature increase in the range 20–100 C. Above 100 C, the relative decrease in strain is believed to be due to the partial hydrolysis of wood by acetic acid and formic acid, as discussed previously (Koran et al. 1978).

Figure 4A further shows that the shear strengths of spruce and balsam fir are practically identical, in spite of their differences in strain (Fig. 4B). It is apparent that the strain values of spruce are 25% higher than those of balsam fir. This means that under the same conditions, balsam fir is significantly more rigid than red spruce. On the basis of its higher rigidity, balsam fir is expected to behave differently from spruce between the refiner plates under the same conditions. The high shive content, for example, obtained in the thermomechanical pulping of balsam fir could well be attributed to its comparatively rigid nature.

Torsional failure in a wooden bar

When a cylindrical member is subjected to torsional loading, there are four types of stresses developed in it. These are τ_L, τ_t, σ_t, σ_c (Fig. 1B). Any one of these stresses can cause failure in a member, depending on its structure and composition. A brittle bar, for example, such as chalk, is known to fail on a 45° helix (Fig. 1B; broken line), owing to the action of the tensile stresses (σ_t) produced at 45° by the applied torque. In contrast, a ductile material, such as an aluminum alloy, fails under the action of the transverse shear stress (τ_t) in the transverse plane (TP; Fig. 1B) at a right angle to the shaft axis. In comparison, a thin-walled hollow member is likely to fail by buckling under the action of the diagonal compressive stresses (σ_c). Wood produces a fourth type of failure; in this case there are two additional factors to be considered. First, wood is a heterogeneous and anisotropic material, that possesses distinctly different structures in its transverse, radial, and tangential planes. Consequently, its strength properties vary accordingly. Its shear strength, for example, is considerably greater in the transverse plane (TP; Fig. 1B) than in the longitudinal plane.

Secondly, the ductility of wood changes considerably with a change in moisture content and temperature. Such a change is most pronounced in the range 50–120 C, where wood becomes progressively more plastic at higher temperatures. The torque-deformation curves shown in Fig. 3 demonstrate this phenomenon along with the strain curves of Fig. 4B.

Plane of fracture in torsional loading

During elastic loadings (OT_0; Fig. 2), the torque is linearly proportional to the angular deformation. In contrast, in the elasto-plastic range (T_0T_1), the wooden bar is permanently deformed. Once the applied torque, T_1 (Fig. 1B), exceeds the shearing elastic-limit of the bar, it fails at T_1 and the torsional load falls back to a lower value (Fig. 3). According to Fig. 3, the failure occurs at an average twist angle of 30.5°.

Microscopic examination of a failure plane reveals that the fracture occurs

almost exclusively in the longitudinal plane, parallel with the grain direction. This fracture is caused by the longitudinal shear stress, τ_L (Fig. 1B), since its plane of action coincides most closely with the grain direction in wood.

Microscopic studies have further shown that the predominant zone of failure occurs in the radial plane of wood. A typical example is shown in Fig. 2. It is evident that the fracture path falls between radial rows of fibers and follows the ray crossings. This is expected, since wood is the weakest in the radial-longitudinal plane.

It was further observed that the initial failure occurs in the outer regions of the cylindrical bar in the form of checks and splits of different sizes. Progressively fewer checks can be found towards the central regions of the shaft.

REFERENCES

ATACK, D. 1980. Towards a theory of refiner mechanical pulping. Appita 34(3):223–227.

GORING, D. A. I. 1963. Thermal softening of lignin, hemicellulose, and lignin. Pulp Paper Mag. Can. 64(12):T517–527.

HOGLUND, H., AND G. TISTAD. 1973. Energy uptake by wood in the mechanical pulping process. *In:* Proceedings of the International Mechanical Pulping Conference, Stockholm, Sweden, June 18–21. Pp. 3:1–3:26.

———, U. SOHLIN, AND G. TISTAD. 1976. Physical properties of wood in relation to chip refining. Tappi 59(6):144–147.

KORAN, Z. 1966. Electron microscopy of black spruce fibre surfaces. PPRIC Technical Report 472. 37 pp.

———. 1967a. Some aspects of mechanical separation of wood fibers. Pulp and Paper Res. Inst. of Canada. Trend 11:14–18.

———. 1976b. Electron microscopy of radial tracheid surfaces of spruce separated by tensile failure at various temperatures. Tappi 50(2):60–67.

———. 1968. Electron microscopy of tangential tracheid surface of black spruce produced by tensile failure at various temperatures. Sven. Paperstidn. 71(17):567–576.

———. 1970. Surface structure of thermomechanical pulp fibers studied by electron microscopy. Wood Fiber 2(3):247–258.

———. 1979. Tensile properties of spruce under different conditions. Wood Fiber 11(1):38–49.

———. 1981. Energy consumption in mechanical fiber separation as a function of temperature. Pulp Paper Can. 82(6):113. Transactions of the Technical Section 7(2):TR11–17.

———, B. V. KOKTA, J. L. VALADE, AND K. N. LAW. 1978. Fiber characteristics of masonite pulp. Pulp Paper Can. 79(3):T107–113.

VIKSTROM, B., AND L. S. HAMMAR. 1979. Defibration in chemimechanical pulping. Sven. Paperstidn. 82(6):171–177.

———, AND P. NELSON. 1980. Mechanical properties of chemically treated wood and chemimechanical pulps. Tappi 63(3):87–91.